18. THE ROLE OF MICROCRACKING ON FRACTURE TOUGHNESS OF BRITTLE COMPOSITES

F.E. Buresch

KFA Jülich, Institut für Reaktorwerkstoffe

1. INTRODUCTION

Ceramic based composites such as carbon reinforced graphite, silicon-based ceramics or zirconia doped alumina are widely expected to provide the next major advance in materials, beyond superalloys and oriented entectics, in enabling a discontinuous increase in the performance of turbines and other heat engines, e.g. HTR-nuclear power stations. Notable progress has been made in overcoming fabrication difficulties and mechanical deficiencies stemming from high-temperature stress-dependent kinetic processes in phase-pure silicon carbide and silicon nitride. Hetero-phase versions of these materials are also attractive. Through processes which utilize alumina as a matrix and unstabelized zirconia particles as the dispersed phase, a wide range of materials with a high toughness and thermo-shock resistance are developed. In these materials a high density of microcracks or microflows are responsible for the attractive thermo-mechanical performance. Microcracking, through an enhancement of the strain-at-fracture can lead especially to a major increase in thermal stress resistance. Increase in the fracture toughness and a general stable mode of crack propagation in microcracked materials also promote thermal stress damage resistance in combination with excellent thermal insulating properties.

2. CRACK PROPAGATION IN CERAMIC BASED COMPOSITES

In brittle polycrystalline materials such as graphite or alumina and many brittle composites macrocrack propagation occurs at an average velocity, determined by the applied macroscopic stress intensity factor K_I and a specified environment and temperature. On the microstructural level, however, we presume that the crack moves intermittently in abrupt increments. This is due to the activation of potential microcrack sites, the grow of this microcracks up to metastable barriers and the coalescence of microcracks to join the macrocrack. The microcracking on the microstructural level is governed by the strength of microstructural stress concentrators and the effective surface energy for trans- or intergranular fracture respectively. A characteristic parameter for this features is the microscopic stress intensity factor k_{Ic}.

Evidence for microcracking during stressing a ceramic by direct and indirect experimental observations is often found in the literature. Specially microscopic observations reveal that the major crack front follows a tortuous path through ceramics and many secondary microcracks branches opened up ahead of and adjacent to the macrocrack front. The macrocrack jumps in discret steps caused by the coincidence alignment of favorable oriented micro-

cracks in the region ahead of the macrocrack.

Typical materials with intense microcracking ahead of a macrocrack have matrix grains with an anisotropic structure like alumina or graphite or those are doped with second phase dispersions. In all these cases microcracking occurs as a consequence of thermal and elastic mismatch in grain boundaries between grains of different orientation or structure. As a result residual strains cause tensile stresses in grain boundary regions. A useful quantity of these stresses is the microscopic stress intensity factor

$$k_{IA} = \frac{E\,\varepsilon}{\sqrt{12\pi}\,(1-\nu^2)}\,\sqrt{d} \qquad (1)$$

which relates the residual stresses $E\varepsilon$ to the square root of the grain size d. If k_{IA} reaches the value of the critical material specific microscopic stress intensity factor k_{Ic} which is related to the specific grain boundary fracture energy through $\sqrt{E\,\gamma_s}$ microcracking will occur /1/.

Most important are residual strains caused by the difference of the coefficients of thermal expansion between adjacent grains. As an example $\varepsilon = \Delta\alpha\,\Delta T$ is in the range of $\sim 10^{-3}$ for alumina. The temperature difference depends on the freezing temperature. It is between 800 and 1200 °C for alumina. Above this temperature all residual strains are vanished by creep.

During loading a ceramic component macrostress superimposed the residual stress. As a consequence microcracking occurs predominantly in the high stressed non-linear elastic zone - called the process zone - ahead of the macrocrack and ceramics acquire their strength and toughness by these dissipative processes.

For understanding the influence of microcracking in the non-linear deformed process zone ahead of the macrocrack front on crack propagation we have introduced the concept of the critical stored elastic energy density and the critical elastic energy release rate of the material inside the process zone as a consequence of a critical microcrack configuration in this region. Furthermore, we have elaborated on an analysis concerning the need of dissipative energy for microcracking inside the process zone. The equations we have worked out provide evidence for the correlation between the stress intensity factor and the critical energy release rate with specific microstructural features (grain size, microcrack density, elastic microcrack interaction, etc.) respectively; they are in agreement with our experimental results. We expect the model to be a usefule tool in aiding the development of ceramics with tailor-made microstructure.

2.1 THE TWIN-PARAMETER APPROACH TO BRITTLE FRACTURE PHENOMENA

The twin-parameter approach of notch fracture mechanics opens the possibility for better understanding of brittle fracture phenomena by introducing a material specific stress intensity factor depending on microstructural parameters. Following Neuber, Weiss, Erismann and Buresch /2-6/ it can be

demonstrated that the fracture of a certain ceramic is determined by critical values for the notch fracture stress σ_{mc} and the size of the process zone ρ_c. It means that the microcrack region in the immediate vicinity of a crack tip is responsible for the non-linear behaviour of ceramics /2-6/.

The non-linear behaviour in front of a crack or notch is governed by the microstructure, especially the grain and pore size distribution and microscopic fracture energy. We will compare quantitatively the change in stored elastic energy during microcracking inside ρ_c with the dissipative energy needed for the generation of microcracks. We neglect other terms of dissipative energy like dislocation motion, glide of crack faces or chemical reactions. With the number of grains in the unit of volume proportional to d^{-3} and the surface energy for a penny-shaped crack proportional to $\gamma_s d^2$ the total dissipative surface energy inside ρ_c is given by

$$W_d = \frac{\pi \rho_c^2 \gamma_s \beta}{2 w d} \tag{2}$$

The symbols β and w denote the part of grains with microcrack and orientation of the microcracks with respect to the main normal stress respectively. β denotes alternatively the concentration of dispersions which generate microcracks as a consequence of thermal expansion mismatch or phase transformation.

In our model it is assued that microcracking will occur if the notch fracture stress reaches the critical value σ_{mc}, lowering the Young's modulus to E_ρ. Then the change in stored elastic energy is given by

$$\Delta W_{ec} = \frac{\pi \rho_c^2 \sigma_{mc}^2 A(v)}{16 E} \left(\frac{1}{f_\rho} - 1\right) \tag{3}$$

It follows with Equations (2) and (3) for critical values of notch fracture stress, stress intensity factor and energy release rate.

$$\sigma_{mc} = 4 \sqrt{\frac{\gamma_s E}{dA(v)} \frac{\beta}{w} \frac{f_\rho}{1-f_\rho}} \tag{4}$$

$$K_{Ic} = 2 \sqrt{\frac{\pi \rho_c \gamma_s E}{dA(v)} \frac{\beta}{w} \frac{f_\rho}{1-f_\rho}} \tag{5}$$

and

$$G_{Ic} = 4 \frac{\pi \rho_c \gamma_s \beta f_\rho}{d A(v) w(1-f)} \tag{6}$$

The term

$$I_\rho = \sqrt{\frac{\beta}{w} \frac{f_\rho}{1-f_\rho}} \tag{7}$$

is the elastic microcrack interaction parameter which denotes the change in stress intensity of one microcrack with respect to the elastic potential of the surrounding microcracks.

The elastic microcrack interaction is well known for an elastic solid by a rectangular array of cracks by Delameter et al. The weakening of the solid can be expressed by

$$\frac{E_\rho}{E} = f_\rho = \frac{1}{1 + \frac{2\pi a_m^2}{xy} B^*(\beta)} \tag{8}$$

where x and y denote the distance of microcracks in rows and stacks respectively. $B^*(\beta)$ is listed for several values of $y/2a_m$ and $x/2a_m$. B^* for a single row of cracks (that is when $y/2a \to \infty$) as a function of x/a_m is found by the expression

$$B^* = 2 \left(\frac{x}{\pi a_m}\right)^2 \ln \left(\sec \frac{\pi a}{x}\right) \tag{9}$$

which is the well known equation for a row of collinear cracks /7/.

Neglecting the difference in density of a three- and two-dimensional array of microcracks, the elastic microcrack interaction parameter equation (7) can approximately be given by

$$\sqrt{\frac{\beta}{w} \frac{f_\rho}{1-f}} = \sqrt{\frac{2}{\pi B^*(\beta)}} \tag{10}$$

This is shown in Figure 1 for a rectangular array of microcracks of different densities. Only a parallel array of microcracks enhance the elastic microcrack interaction parameter.

3. INFLUENCE OF MICROCRACKING ON THE TOUGHNESS OF COMPOSITES

It is of great interest to prove the usefulness of the present theory with data known from the literature. Alumina ceramics doped with unstabelized zirconia particles have a very high toughness. This has been shown by Dworak, Claussen, Garvie and others /8-11/. The enhanced toughness is a consequence of a high density of microcracks and their elastic interaction inside the non-linear deformed process zone.

The microcracks are a consequence of residual stresses caused by thermal mismatch and phase transformation of unstabelized zirconia particles in

the fine grained alumina matrix. The microscopic stress intensity factor for these residual stresses lies in the range of 1 MPa $m^{1/2}$ depending on the size of the zirconia particles. Thus the residual strain induced microscopic stress intensity factor exceeds the critical specific microscopic stress intensity factor causing spontaneous microcracking during cooling from the sintering temperature. (See also /1/).

Following the experimtal observations of Claussen and coworkers /9,10/ we will compute qualitatively the microcrack density inside the process zone of these composites. With this value we will estimate the value of the elastic microcrack interaction parameter.

Figure 2 shows in the upper part measurements of Claussen et al. about the dependence of toughness and bend strength on the volume fraction of zirconia particles of different sizes. The particle size data refer to sub-sieve size tests but in their paper the authors have remarked that the actual particle size found in the hot pressed composites was by a factor of three larger due to agglomeration during mixing the powder and forming the specimens.

As shown in Figure 2 the fracture toughness increases with decreasing particle size and increasing volume fraction of particles up to a critical maximum value. The peaks of maximum values increase with decreasing particle size and shift to higher volume fractions. With increasing volume fractions of particles beyond the critical maximum value, the toughness drops sharply for all particle sizes.

The upper right diagram shows the bend strength of these composites. Generally the bend strength increases with decreasing particle size. For each particle size the bend strength remains nearly constant with increasing volume fractions of particles up to the critical value V_{dc} corresponding to the peak value of the fracture toughness curve. The bend strength decrease sharply like the toughness of volume fractions beyond the critical value.

We will look for the influence of density and elastic interaction of microcracks inside the process zone on fracture toughness of these composites. It can be shown, that the features are corresponding to the present theory.

The observed features - the decrease of K_{Ic} with the particle size and its increase with volume fraction of particles - are governed by the size density and elastic interaction of the microcracks which are generated in these systems as a consequence of the thermal and elastic mismatch and the phase transformation of the particles. The size of the microcracks depend on the available fracture energy rate. For an unloaded specimen the microcrack size is proportional to the particle size because the residual strain induced energy rate is also proportional to that particle size.

For the loaded specimen the microcrack size is depending on both the residual strain energy and the stored bulk volume elastic energy as well as on the elastic interaction of the microcracks inside the process zone. These facts are shown in the lower part of Figure 2.

The peak values of fracture toughness for a specific particle size can be explained in terms of the present theorey as a critical value of the elastic microcrack interaction parameter. That means this value characterizes the highest energy density which can be achieved inside the process zone for the specific composite. This value is defined by a critical value V_{dc}

of volume fraction of zirconia particles. The drop of the toughness beyond this value is caused by junction of microcracks. The critical maximum size and density of microcracks which are responsible for the peak value can be computed using appropriate formulas. We will compute first the average interparticle spacing X_d as suggested by Koks who used a basis like the mean square root of the area per particle, i.e. /12/

$$X_d = N_\Delta^{-\frac{1}{2}} \tag{11}$$

where N_Δ is the number of particles per unit area. For a random array of spherical particles, size d, the expression becomes

$$X_d = d \left[\sqrt{\frac{2\pi}{3\,V_d}} - \frac{\pi}{2} \right] \tag{12}$$

where V_d is the volume fraction of particles and the correction term accounts for the finite size of the particles. To transfer this formula to the intermicrocrack spacing it is assumed that each particle is responsible only for one microcrack. This follows also from energy considerations.

The interparticle spacing as a function of the volume fraction of particles for the four measured effective particle size as parameter is plotted on the lower left side of Figure 2. Following the experimental observations of Claussen et al., three times the diameter denoted in the upper diagram is used in rounded numbers /9/.

The critical volume fractions of particles for the peak values of toughness characterize a critical interparticle spacing which is given by the dotted curve (denoted I) in the lower left diagram. This spacing is aquivalent to the average maximum microcrack size. The lower right diagram shows the microcrack densities for the microcrack sizes in question as a function of the volume fraction of particles. The critical microcrack density is plotted with the dotted durve denoted II. The most interesting result shows that for each particle size the critical microcrack density of the peak value of toughness is constant for all volume fractions about one. That means the microcrack density is about 50 % as pointed out by Hoagland and coworkers /13/.

The microcracks inside the process zone of these composites are mostly arranged perpendicular to the applied stress. That means they are arranged in a fashion which can be compared with an orthogonal array of rows and stacks of microcracks. The elastic interaction of such array of microcracks was computed by Delameter et al. as shown in the previous section (Fig. 1).

We can guess that the value of the critical microcrack interaction parameter for the peak value of toughness of the composites lies for all composites in the range of one to two. But this is not the final result. In an early paper /5/ we have computed values of I_ρ of different technical aluminas using measured values for K_{Ic}, ρ_c and other microstructural parameters. This values as a function of K_{Ic} are shown in the next Figure 3. For a K_{Ic} of about 5 which corresponds to the value for the undoped alumina

ceramics of Claussen et al., I_ρ has a value of about 0.5. That means doubling the value of I_ρ of the undoped material gives an estimate of the value of K_{Ic} of the composites. But this must be proved by further works.

Finally it is of interest to look for the influence of the microcrack density of undoped ceramics on the fracture toughness of these materials and to ask for the minimum particles concentration which must be introduced to get an increase in toughness. With this respect two classes of dispersion toughened composites should be compared: one with a polycristalline matrix, the other with a glass matrix. Figures 4 and 5 show a replot of toughness values for these two classes of composites /8-11, 14/ as a function of dispersion density. The microcrack density varies from the dispersion density by a factor of n (see Figure 2). Only values for the increase of toughness with increasing volume fraction of particles are introduced. The regions denoted as I, II and III characterize values of maximum toughness with respect to particle sizes.

It can be seen from these figures that the "ground level of microcracks" in the polycristalline based composites lies in the density range of about 0.1 to 0.5 whereas in the glass based composites the microcrack density of the undoped material is zero. This is not unexpected. The results show that at instability the process zone of an alumina base specimen with respect to the specific microstructure contents about some ten microcracks if we assume that the size of the process zone is about 20 grain sizes /6/. However, it must be pointed out that the size of the process zone depends markedly on the Weibull-modulus and also on the value of the microscopic stress intensity factor k_{Ic}. In a glass base specimen a real process zone does not exist. Furthermore it can be concluded that the increase in toughness of these materials with increasing microcrack density, i.e. particle density, is mainly a consequence of a parallel array of microcracks inside the non-linear deformed process zone.

4. Discussion

For a specific ceramic with values E and γ_s for Young's modulus and inter- or transgranular fracture energy respectively the fracture toughness is governed by the length, density and elastic interaction of the microcracks in the non linear deformed process zone. It is well known from literature (see e.g. /15/) that, for various arrangements of microcracks, the parallel array of microcracks strengthens and conversly the collinear array of microcracks softens brittle material. The interaction effect of parallel oriented microcracks is much stronger as that of collinear microcracks as shown in Fig. 1 (see also /15/). Only the interaction effect of a small number of microcracks is computed in the literature because of complexity of the calculations /15/. However, in the present model we consider the overall influence of a great number of microcracks on the elastic properties of the material

in the process zone. Thus we do not need to compute the interaction effect of an individual microcrack with respect to the surrounding microcracks.

As a base for the computations to investigate the change of elastic properties of a brittle material with regard to microcracking we have visualyzed an infinite elastic solid containing a doubly periaodic rectangular array of slitlike cracks. These computations are worked out by Delameter et al /7/. With these we have computed the change of elastic properties with density of an orthogonal array of microcracks hold for an infinite body. Thus for the specific case of a process zone of finite size random effects may influence the result. However, for a first approximation our results show that the toughness of zirconia doped alumina is governed by the elastic interaction of a high density of microcracks in the process zone. The elastic microcrack interaction parameter I_ρ is nearly constant irrespective of the length of the microcracks (Fig. 2). Thus, we will compare the peak value of toughness for composites with different volume fraction and size of dispersions for constant values for the elastic microcrack interaction parameter I_ρ (Fig. 2) assuming constant values for the size of the process zone ρ_c and as a first approximation also for E and γ_s. With the critical length of the microcracks denoted in Fig. 2, applying eq. (5) the ratio of these toughness values is given by the equation

$$K_{Ic}(6{,}4\ \mu m) : K_{Ic}(2{,}85\ \mu m) : K_{Ic}(1{,}75\ \mu m) : K_{Ic}(1{,}25\ \mu m) = \frac{1}{\sqrt{110}} : \frac{1}{\sqrt{30}} : \frac{1}{\sqrt{16}} : \frac{1}{\sqrt{9}} \qquad (13)$$

or in rounded numbers

$$0{,}6 : 0{,}75 : 0{,}8 : 1 \approx 0{,}03 : 0{,}55 : 0{,}76 : 1$$

Within the limits of the approximations made for these computations, the result shows the usefulness of the present theory to explain the mechanisms which govern the fracture toughness of these dispersion toughened composites.

LITERATURE

1. Buresch, F.E. Science of Ceramics 7, 1973, 383 and 475
2. Neuber, H. Kerbspannungslehre Springer Vlg. 1958
3. Weiss, V. Fracture III. Academic Press, N.Y. 1971, 227
4. Erismann, T. H. Material und Technik, 1973, 120
5. Buresch, F. E. Fracture Mechanics of Ceramics, Vol 4, 1978, 835-847
6. Buresch, F. E. A.S.T.M.-S.T.P. in press
7. Delameter, W. R., Hermann, G. and Barnett, D. M. Trans. ASME 1975, 74
8. Dworak, U., Olapinski, H. und Tamerus, G. Ber.D.K.G. 55, 1978, 98-101
9. Claussen, N., Steeb, J., Pabst, R. Jour. Amer. Ceram. Soc. 56, 1977, 559-562
10 Claussen, N. Jour. Amer. Ceram. Soc. 59, 1976, 49-51
11 Garvic, R. C., Hannink, R. H. and Pascoe R. T. Nature 258, 12, 1975, 703
12 Kocks, U. F. Acta. Met. 14, 1966, 1629
13 Hoagland, R. G., Embury, J. D. and Green, D. Y. Scripta Metallurgica 9, 1975, 907
14 Swearengen, J. C., Beauchamps, E. K. and Bagan, R.J. Fracture Mechanics of Ceramics, Vol 4, 1978, 873-892
15 Radwani, M. Rep. IFKM 5/72

List of Figures

Fig. 1: Correlation of Theoretical Elastic Microcrack Interaction Parameter

$$I_\rho = \sqrt{\beta \frac{f_\rho}{1-f_\rho}} = \sigma_{mc} \sqrt{\frac{a_m A(\nu)}{\gamma_s E}} \approx \sqrt{\frac{2}{\pi B^+(\beta)}}$$

with Microcrack Density (Values of B^+ (β) are listed by Delameter et al, 1975) /7/.

Fig. 2: Fracture Toughness, Microcrack Length and Microcrack Density of Zirconia Doped Alumina.

Fig. 3: Elastic Microcrack Interaction Parameter (Experimental) of Two Aluminas as a Funktion of Their Stress Intensity Factors. (Figures in Parenthesis are Mean Grain Size in µm and Densities in kg/m^3) /5/.

Fig. 4: Replot of Fracture Toughness Values of ZrO_2-Dispersions Toughened Alumina (after Claussen et al /9/) as Function of Dispersion Density.

Fig. 5: Replot of Fracture Toughness Values of Dispersion Toughened SiO_2-Glasses. (Reinforced with Spherical Polycristalline Al_2O_3 Particles, Sized 25 µm). The Figures Denote the Molar Ratios of B_2O_3 and Na_2O (after Swearengen et al /14/)

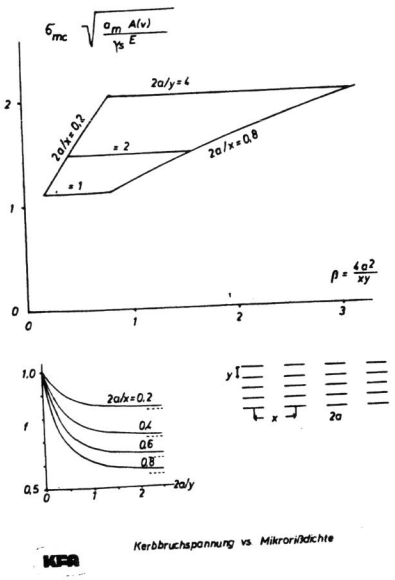

Kerbbruchspannung vs. Mikrorißdichte

KfA

Fig. 1

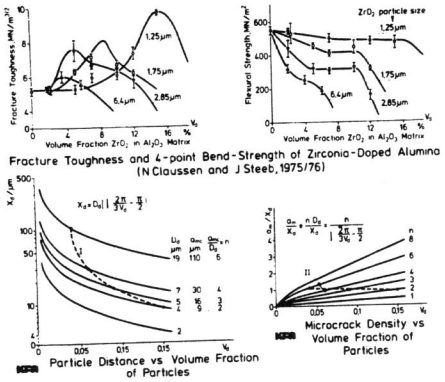

Fracture Toughness and 4-point Bend-Strength of Zirconia-Doped Alumina (N.Claussen and J.Steeb, 1975/76)

KfA

Fig. 2

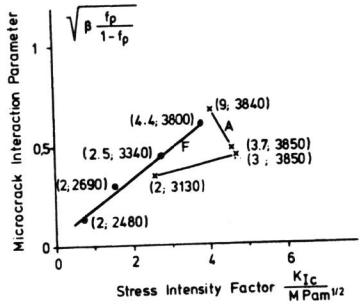

KfA Elastic Microcrack Interaction Parameter (Experimental) of Two Aluminas as a Function of their Stress Intensity Factors. (Figures in paranthesis are mean grainsizes in µm and densities in kg/m^3)

Fig. 3

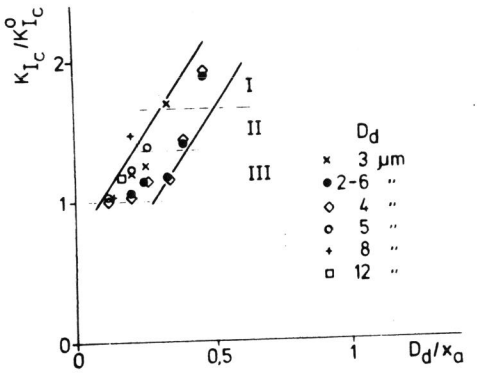
K_{Ic}/K^{o}_{Ic}
2
1
0
0
0,5
1
D_d/x_a
I
II
III
D_d
× 3 µm
● 2-6 "
◇ 4 "
○ 5 "
+ 8 "
□ 12 "

Fig. 4

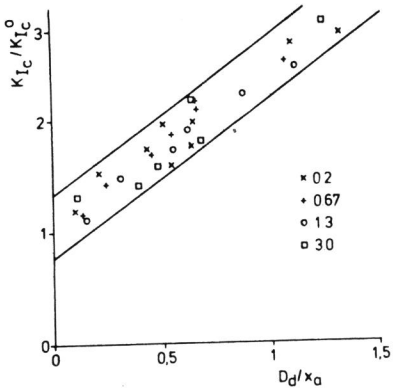
K_{Ic}/K^{o}_{Ic}
3
2
1
0
0
0,5
1
1,5
D_d/x_a
× 0.2
+ 0.67
○ 1.3
□ 3.0

Fig. 5